MAGNETIC RESONANCE IN MEDICINE 1, 502–507 (1984)

Driven-Equilibrium Radiofrequency Pulses in NMR Imaging

C. M. J. VAN UIJEN AND J. H. DEN BOEF

Philips Research Laboratories, P.O. Box 80,000, 5600 JA Eindhoven, The Netherlands

Received April 13, 1984

Driven-equilibrium pulse techniques are applied to NMR imaging to extend the possibilities of manipulating image contrasts in pulse sequences with a high repetition rate. In many cases the data acquisition time can be much shorter than in more conventional pulse techniques. Both calculations and experiments reveal that the intensity of tissue with slowly relaxing nuclear magnetizations can significantly be enhanced, thus facilitating the detection of a number of pathologies.

INTRODUCTION

Apart from requirements on resolution and signal-to-noise ratio, the total time for data acquisition in NMR imaging is determined by the repetition rate at which the spin system is excited. In the early days of NMR imaging, an almost complete return of the nuclear magnetizations to equilibrium preceded each excitation. This was done to prevent significant signal loss in an imaging technique with inherent low sensitivity. The steady-state free-precession pulse technique, first described by Carr (*1*) and applied to NMR imaging by Hinshaw (*2*), deviated from this idea, but good images were nevertheless produced because the signal reduction was not too dramatic and many averages could be taken within a reasonable time. The technique has fallen into disuse, since it requires the projection–reconstruction approach to spatially encode the NMR signals and consequently it is more sensitive to magnetic field inhomogeneities than Fourier imaging. It is noted that in the steady-state free-precession technique the response of the system virtually depends on the *ratio* of the longitudinal and transverse relaxation times T_1 and T_2. This ratio is nearly the same in many tissues and thus the contrast in the NMR images is reduced.

In imaging techniques using the more conventional radiofrequency pulse sequences it also appeared to be advantageous to drop the idea of maximum response, since the contrast-to-noise rather than the signal-to-noise ratio determines the clinical importance of the image, as is convincingly shown in images obtained with an inversion–recovery pulse sequence. In a saturation–recovery experiment it is therefore often preferred to use a rather short recovery time, say 0.5 sec or less. This, of course, has the additional advantage that the imaging time is relatively short. However, it significantly decreases the NMR signal of tissues with a long T_1, and consequently contrast is lost with tissues having a low concentration of NMR-active nuclei. Since T_1 increases with the rf frequency, the effect is stronger at the higher fields.

0740-3194/84 $3.00

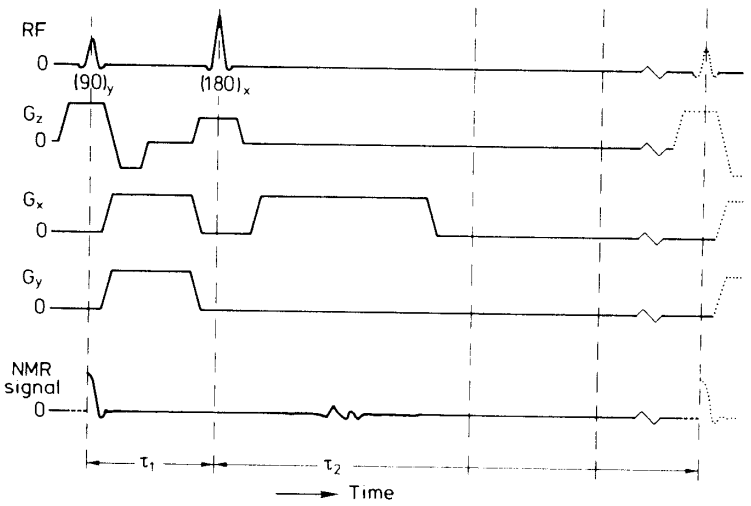

FIG. 1. Radiofrequency pulse sequence for a saturation–recovery experiment using a spin-echo technique. The gradient-pulse scheme refers to Fourier imaging of a (pseudo) 2-D xy plane, with G_α ($\alpha = x, y, z$) denoting the gradient in the α direction.

In this paper we discuss the application of driven-equilibrium rf pulse techniques (*3*)[1] in NMR imaging, and show that it can be used to recover this contrast without increasing the recovery time.

DESCRIPTION OF THE METHOD

The technique relies on the fact that, after data collection, application of a 180° rf spin-echo pulse and properly adjusted field gradients refocuses the transverse nuclear magnetizations so that they can easily be reoriented by a resonant rf pulse. In particular, these magnetizations can be set along the equilibrium direction, and the resonant pulse is then often referred to as driven-equilibrium pulse. The procedure is applicable to all currently used rf pulse sequences and imaging techniques, but the discussion in this paper is restricted to two-dimensional (2-D) Fourier imaging where in every pulse sequence only one spin echo is generated. A typical gradient and rf pulse sequence for such an experiment is given in Fig. 1. Figure 2 shows the modifications of this scheme required for the implementation of a driven-equilibrium pulse. A second echo is generated and gradients are applied in such a way that at the point of this echo dephasing effects due to previously applied gradients cancel. At this point a 90° rf pulse is then applied to rotate the total transverse magnetization **M** toward the direction of the static magnetic field $\mathbf{B}_0$. It is noted that other flip angles can be used as well, and that it is even possible to set the magnetization antiparallel to the field, because the rotation depends on the phase of the 90° pulse in conjunction with the phases of previously applied rf pulses. For example, a $(90°)_y$–$(180°)_x$–$(180°)_x$–$(90°)_{-y}$ pulse sequence rotates **M** toward $\mathbf{B}_0$, whereas $(90°)_y$–$(180°)_x$–$(180°)_x$–$(90°)_y$ sets the magnetization antiparallel

[1] A preliminary account of this work was presented at the Second Annual Scientific Meeting of the Society of Magnetic Resonance in Medicine, San Francisco, August 16–19, 1983. The abstract appeared in *Magn. Reson. Med.* **1**, 268 (1984).

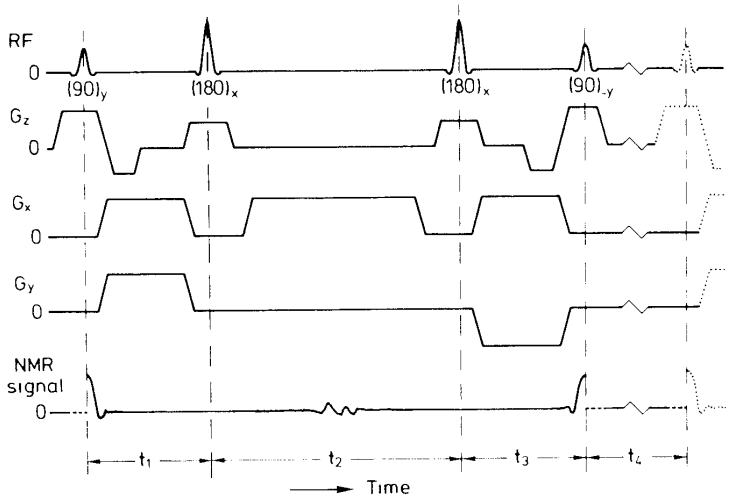

FIG. 2. A driven-equilibrium rf and gradient-pulse scheme for 2-D Fourier imaging.

to $\mathbf{B}_0$. It is further noted that when the initial excitation is spatially selective, the second 90° pulse is preferably selective as well. This reduces the possibility of generating signals emerging from parts of the object outside the region of interest.

It is obvious that the effect of the driven-equilibrium pulse depends on the relaxation times T_1 and T_2. For example, magnetizations with very short T_2 and long T_1 have, to a great extent, lost their transverse components at the point of second echo, and virtually no effect will occur. To quantify this, we have calculated the steady-state response of the system at the point of first echo for the pulse sequence shown in Fig. 2. The result, assuming uniexponential relaxation, reads

$$S^{\mathrm{DE}} = kM_0 \frac{1 - \exp(-t_4/T_1)}{1 - \exp[-(t_1 + t_2 + t_3)/T_2] \exp(-t_4/T_1)} \exp(-2t_1/T_2) \qquad [1]$$

where t_i ($i = 1, 2, 3, 4$) is defined in Fig. 2, and DE is shorthand for driven equilibrium. Further, M_0 is the equilibrium magnetization and k represents the instrumental parameters. For $t_i \ll T_1, T_2$, Eq. [1] is approximated by

$$S^{\mathrm{DE}} \approx kM_0 \frac{1}{1 + (T_1/T_2)(t_1 + t_2 + t_3)/t_4}. \qquad [2]$$

Note that, because of the dependence on the ratio T_1/T_2, there is similarity with the steady-state free-precession technique. For the saturation–recovery sequence (Fig. 1), we have

$$S^{\mathrm{SR}} = kM_0\{1 - 2\exp(-\tau_2/T_1) + \exp[-(\tau_1 + \tau_2)/T_1]\} \exp(-2\tau_1/T_2) \qquad [3]$$

where it is assumed that due to field inhomogeneities complete dephasing of the magnetizations occurs during the interval τ_2. For $\tau_i \ll T_1, T_2$,

$$S^{\mathrm{SR}} \approx kM_0 \frac{\tau_2 - \tau_1}{T_1}. \qquad [4]$$

Note that in this case $S^{SR} \ll kM_0$, while for $t_4 \gg t_1 + t_2 + t_3$ and $T_1 = T_2$, Eq. [2] gives $S^{DE} \approx kM_0$.

RESULTS AND DISCUSSION

Figure 3a shows an application of the driven-equilibrium pulse in NMR imaging. The result is obtained in a resistive magnet operating at 0.14 T, and, like the rest of the images shown in this paper, a slice of 1 cm thickness is imaged on a 128×128 matrix by 2-D Fourier imaging. The interpulse times are $t_1 = t_3 = 25$ msec, $t_2 = 50$ msec, and $t_4 = 210$ msec. For comparison, the saturation–recovery result is shown in Fig. 3b, where $\tau_1 = 25$ msec and $\tau_2 = 285$ msec were chosen to get the same pulse-sequence repetition rate. Note the enhanced contrast between tissue with high proton concentration and long T_1 and T_2 and tissue with low proton concentration, which explains why in Fig. 3a the eye lens can clearly be distinguished. This will probably also facilitate the visualisation of a slipped disc by NMR. It is further noted that blood vessels appear dark in Fig. 3a, because in moving parts of the object the rephasing of the magnetizations in the driven-equilibrium pulse sequence is in general incomplete, resulting in a reduced effect of the driven-equilibrium rf pulse. As a consequence, contrast is obtained with tissue having a high proton concentration and long T_1 and T_2. This is not the case in Fig. 3b where, cf. Eq. [4], both types of tissue appear dark. Here probably lies another important application of the technique.

As already stated, it is also possible to rotate the transverse magnetizations to the direction antiparallel to $\mathbf{B}_0$. It is known from inversion–recovery experiments that this can give interesting contrasts in the images. At this point, it is important to realize that in the initial selective excitation the flip angle varies over the slice

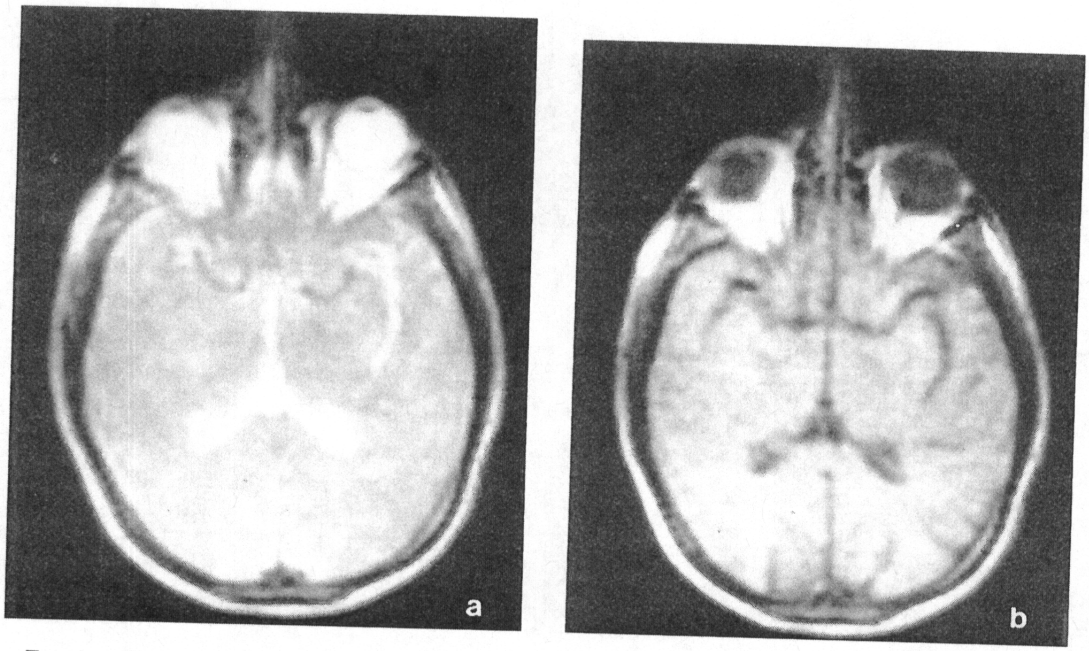

FIG. 3. (a) NMR image of a 1 cm thick slice of a human head using the driven-equilbrium sequence sketched in Fig. 2. To increase the signal-to-noise ratio, every NMR profile was detected twice. With a pulse-sequence repetition time of 310 msec, it took about 80 sec to record this $(128)^2$ image. (b) Image of the same slice as in Fig. 3a, but obtained with the rf sequence shown in Fig. 1. The imaging time was again 80 sec.

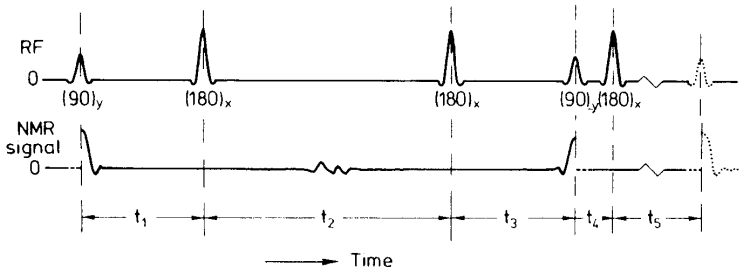

FIG. 4. Radiofrequency pulse sequence for setting the transverse magnetization that is present at the point of the driven-equilibrium pulse antiparallel to the static magnetic field, provided that the magnetization was parallel to this field before the excitation.

thickness and deviates from 90° in large parts of the slice. A second and identical excitation would therefore not properly position the magnetizations antiparallel to $\mathbf{B}_0$. A remedy for this is to first set the magnetizations along the equilibrium direction, thereby automatically correcting for the deviations of the flip angle from 90°, and subsequently to rotate the magnetization over 180° by an rf pulse that is less selective. This procedure results in the rf pulse scheme represented in Fig. 4. New pulse sequences are formed by combining two such sequences with at least

TABLE 1

SIGNAL RESPONSES S_1 AND S_2 IN A COMPOSITE rf-PULSE SCHEME CONSISTING OF TWO CONSECUTIVE (SUB)SEQUENCES OF FIG. 4, BUT WITH DIFFERENT INTERPULSE TIMES t_5, VIZ., t'_5 = 300 msec AND t''_5 = 600 msec[a]

T_1	T_2	S_1	S_2	σ_1	σ_2
3000	3000	33.3	−20.0	26.7	−11.1
	1000	26.4	−12.8	25.8	−10.7
1000	1000	45.4	−6.2	58.4	−7.8
	500	41.2	−2.0	55.5	−7.4
600	400	52.6	9.4	70.2	6.9
	200	45.8	13.2	61.9	6.1
	100	35.9	15.3	48.2	4.8
300	200	64.2	34.4	74.6	37.7
	100	50.7	30.9	58.1	29.3
	50	31.3	21.3	35.2	17.8
100	100	60.4	56.3	60.6	58.4
	50	36.7	34.5	36.8	35.4

[a] Entries for S_1 and S_2 are percentages of kM_0, i.e., percentages of the response of a completely relaxed magnetization. Relaxation times are in milliseconds. S_1 is the signal preceding t'_5, S_2 the signal preceding t''_5. The other interpulse times are $t_1 = t_3 = 25$ msec, $t_2 = 50$ msec, and $t_4 = 11$ msec. For comparison, the right two columns give the results σ_1 and σ_2 for the composite saturation/inversion–recovery sequence with $t_1 = 400$ msec, $\tau_1 = 25$ msec, and $\tau_2 = 1000$ msec. Here, t_1 is the interval between inversion and excitation, and τ_1 and τ_2 are defined in Fig. 1. Entries for σ_1 and σ_2 are again percentages of kM_0.

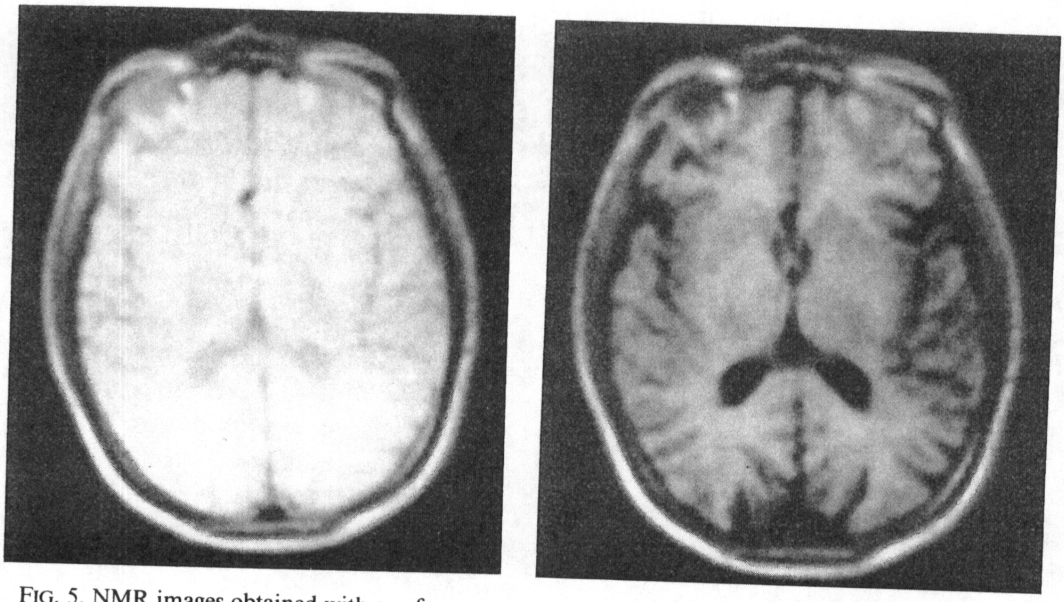

FIG. 5. NMR images obtained with an rf sequence comprising two consecutive (sub)sequences as shown in Fig. 4, but with different values for t_5: t'_5 = 300 msec and t''_5 = 600 msec. The other intervals are $t_1 = t_3$ = 25 msec, t_2 = 50 msec, and t_4 = 11 msec.

one of the interpulse times differing. In each of these subsequences an NMR signal is detected. The contrast in the images obtained from these different data sets can be influenced by varying the interpulse times. For example, results similar to those produced by the combined saturation/inversion–recovery sequence can be obtained. This is best appreciated from the steady-state solution of the Bloch equations. Since the expressions are rather formidable, they are not reproduced here; instead Table 1 gives the outcome of the calculation for an rf scheme consisting of two consecutive (sub)sequences of Fig. 4 with different values for t_5, viz; t'_5 = 300 msec and t''_5 = 600 msec, respectively. The combinations of T_1 and T_2 occurring in Table 1 are thought to cover the values for most of the imaged tissues. For comparison, the results for the saturation/inversion–recovery sequence are also given. Note the resemblance between the responses in both techniques. With the assumed interpulse times, however, the latter requires a 2.2 times longer data acquisition time. Figure 5 gives the results of the composite driven-equilibrium sequence in an actual application.

Of course many variations on the pulse sequences discussed in this paper are possible, and probably by no means all of them are interesting for medical diagnosis. Conclusions on the full importance of the technique thus await applicational research, but it can already be stated that the method significantly extends the possibilities of manipulating the contrasts while maintaining a high repetition rate of the pulse sequence.

REFERENCES

1. H. Y. CARR, *Phys. Rev.* **112,** 1693 (1958).
2. W. S. HINSHAW, *J. Appl. Phys.* **47,** 3709 (1976).
3. See, e.g., J. S. WAUGH, *J. Mol. Spectrosc.* **35,** 298 (1970).